Chem. Mater. **1999,** *11,* 2185−2190

High-Pressure Synthesis and Characterization of a New Series of V-Based Superconductors $(Cu_{0.5}V_{0.5})Sr_2Ca_{n-1}Cu_nO_y$

N. D. Zhigadlo,[†] Y. Anan, T. Asaka, Y. Ishida, Y. Matsui, and E. Takayama-Muromachi*

National Institute for Research in Inorganic Materials (NIRIM), 1−1 Namiki, Tsukuba, Ibaraki, 305-0044, Japan

Received February 22, 1999. Revised Manuscript Received May 20, 1999

A new series of high transition temperature (T_c) superconductors $(Cu,V)Sr_2Ca_{n-1}Cu_nO_y$ [(Cu,V)−12(n − 1)n−Sr, n = 3−7] was synthesized under a high-pressure/high-temperature condition of 6 GPa and 1300 °C. X-ray diffraction and transmission electron microscopy measurements revealed that they have M−12(n − 1)n-type structures with M = (Cu,V) and a stacking sequence of planes, SrO−(Cu,V)O−SrO−CuO_2−$(Ca-CuO_2)_{n-1}$. Simple tetragonal lattices without any superstructures were observed for every member of the series implying a random arrangement of copper and vanadium in the (Cu,V) plane. Electron-probe microanalysis indicated partial substitution of strontium for calcium in the (Cu,V)−12(n − 1)n−Sr phases. All the (Cu,V) phases gave large diamagnetic susceptibilities at a low temperature indicating bulk nature of superconductivity. The highest T_c was found to be 107 K for the (Cu,V)−1234−Sr phase.

1. Introduction

The structures of high transition temperature (T_c) superconductors consist of an alternative stack of a charge reservoir block and an infinite-layer block. Among various kinds of charge reservoirs, an AO−MO−AO type (A: alkaline-earth metal) appears most frequently, forming an $MA_2Ca_{n-1}Cu_nO_{2n+3}$ [M−12(n − 1)n−A] series of superconductors. The M site is not always occupied by one element but is often shared by two or more elements, usually with copper as one element. For several years now, high-pressure synthesis has been recognized to be quite effective for stabilizing the superconducting layered structures, and a large number of $(Cu,M')A_2Ca_{n-1}Cu_nO_y$ [(Cu,M′)−12(n − 1)-n−A] superconductors have been synthesized using this technique.[1]

Recently, a (Cu,Cr)-based series of phases, (Cu,Cr)−12(n − 1)n−Sr, was synthesized under high pressure for n = 1−9; this range of n is the widest among all homologous series ever discovered.[2] The successful preparation of the (Cu,Cr)-based series suggests that other transition metals should be considered as possible candidates for the M′ site of the (Cu,M′) plane. The chromium in the (Cu,Cr) phases is hexavalent and exists as a small cation of Cr^{6+} in the structures.[2] Vanadium looks to be a promising candidate owing to its ability to form a pentavalent ion of V^{5+} with a small size similar to that of Cr^{6+}. Vanadium has been already used as a charge reservoir substituent for mercury in Hg−12(n − 1)n−Ba and thallium in Tl−1212−Sr to discover $(Hg,V)Ba_2Ca_{n-1}Cu_nO_{2n+2+\delta}$ (n = 1,[3] 2,[3] 3[4]) and $(Tl,V)Sr_2CaCu_2O_7$.[5] These studies suggest once more similarity of vanadium and chromium when they are used as a charge reservoir substituent because chromium can also substitute for mercury in Hg−12(n − 1)n−A (A = Sr, Ba)[6−8] and thallium in Tl−12(n − 1)n−A.[9−11]

In a preliminary study, we observed superconducting transitions in high-pressure products of the V−Sr−Ca−Cu−O system.[12] However, superconducting phases were not isolated, and their detailed characterization was not carried out. In the present study, we have performed systematic phase search experiments under a high-pressure/high-temperature condition for the V−Sr−Ca−Cu−O system and succeeded in isolating and identifying the (Cu,V)−12(n − 1)n−Sr series of superconductors which are essentially isostructural to (Cu,Cr)−12(n − 1)n−Sr. Their structural and superconducting properties are reported.

---

* Corresponding author.

[†] NIRIM STA fellow, on leave from Institute of Solid State and Semiconductor Physics, P. Brovki 17, Minsk 220072, Belarus.

(1) Takayama-Muromachi, E. *Chem. Mater.* **1998**, *10*, 2686.
(2) Loureiro, S. M.; Matsui, Y.; Takayama-Muromachi, E. *Physica C* **1998**, *302*, 244.
(3) Maignan, A.; Pelloquin, D.; Hervieu, M.; Michel, C.; Raveau, B. *Physica C* **1995**, *243*, 214.
(4) Maignan, A.; Pelloquin, D.; Malo, S.; Michel, C.; Hervieu, M.; Raveau, B. *Physica C* **1995**, *243*, 233.
(5) Liu, R. S.; Zhou, W.; Edwards, P. P. *Appl. Phys. Lett.* **1990**, *57*, 2492.
(6) Chmaissem, O.; Sheng, Z. Z. *Physica C* **1995**, *242*, 23.
(7) Maignan, A.; Pelloquin, D.; Malo, S.; Michel, C.; Hervieu, M.; Raveau, B. *Physica C* **1995**, *243*, 233.
(8) Shimoyama, J.; Hahakura, S.; Kitazawa, K.; Yamafuji, K.; Kishio, K. *Physica C* **1994**, *224*, 1.
(9) Sheng, Z. Z.; Li, Y. F.; Tang, Y. Q.; Chen, Z. Y.; Pederson, D. O. *Solid State Commun.* **1992**, *83*, 205.
(10) Chen, Z. Y.; Sheng, Z. Z.; Tang, Y. Q.; Li, Y. F.; Wang, L. M.; Pederson, D. O. *Appl. Phys. Lett.* **1993**, *62*, 3034.
(11) Michel, C.; Letouze, F.; Martin, C.; Hervieu, M.; Raveau, B. *Physica C* **1996**, *262*, 159.
(12) Zhigadlo, N. D.; Takayama-Muromachi, E. *Advances in Superconductivity XI*; Proceedings of the 11th International Symposium on Superconductivity; Springer-Verlag: Tokyo, 1998; in press.

10.1021/cm990109+ CCC: $18.00

Table 1. Chemical Compositions of Starting Mixtures, Observed Superconducting Phases, and Superconducting Properties of the High-Pressure Samples

no.	starting composition	observed phases[a]	T_c (K)	χ (10^{-3} emu/g)[b]
1	$Cu_{0.5}V_{0.5}Sr_2CuO_{5.15}$		not superconducting	
2	$Cu_{0.5}V_{0.5}Sr_2CuO_{5.0}$		not superconducting	
3	$Cu_{0.5}V_{0.5}Ca_2CuO_{5.0}$		not superconducting	
4	$Cu_{0.5}V_{0.5}Ca_2CaCu_2O_{7.3}$		not superconducting	
5	$Cu_{0.5}V_{0.5}Sr_2CaCu_2O_{7.6}$	1223	95	−5.64
6	$Cu_{0.5}V_{0.5}Sr_2CaCu_2O_{7.5}$	1223	98	−5.68
7	$Cu_{0.5}V_{0.5}Sr_2CaCu_2O_{7.3}$	1223, 1234	98	−5.88
8	$Cu_{0.5}V_{0.5}Sr_2CaCu_2O_{7.15}$	1234	98	−9.07
9	$Cu_{0.5}V_{0.5}Sr_2CaCu_2O_{7.0}$	1234, 1245	92,72	−5.10
10	$Cu_{0.5}V_{0.5}Sr_2Ca_2Cu_3O_{9.7}$	1234	104	−4.78
11	$Cu_{0.5}V_{0.5}Sr_2Ca_2Cu_3O_{9.6}$	1234	107	−7.17
12	$Cu_{0.5}V_{0.5}Sr_2Ca_2Cu_3O_{9.5}$	1234	105	−7.98
13	$Cu_{0.5}V_{0.5}Sr_2Ca_2Cu_3O_{9.4}$	1245	75	−7.64
14	$Cu_{0.5}V_{0.5}Sr_2Ca_2Cu_3O_{9.3}$	1245, 1256	73	−6.30
15	$Cu_{0.5}V_{0.5}Sr_2Ca_2Cu_3O_{9.2}$	1245, 1256	not measured	
16	$Cu_{0.5}V_{0.5}Sr_2Ca_2Cu_3O_{9.1}$	1256	73	−6.33
17	$Cu_{0.5}V_{0.5}Sr_2Ca_2Cu_3O_{9.0}$	1256	73	−1.58
18	$Cu_{0.5}V_{0.5}Sr_2Ca_3Cu_4O_{11.8}$	1245	not measured	
19	$Cu_{0.5}V_{0.5}Sr_2Ca_3Cu_4O_{11.6}$	1245	75,95	−5.68
20	$Cu_{0.5}V_{0.5}Sr_2Ca_3Cu_4O_{11.4}$	1256	75	−6.64
21	$Cu_{0.5}V_{0.5}Sr_2Ca_3Cu_4O_{11.25}$	1267	not measured	
22	$Cu_{0.5}V_{0.5}Sr_2Ca_3Cu_4O_{11.15}$	1267	73	−5.85
23	$Cu_{0.5}V_{0.5}Sr_2Ca_3Cu_4O_{11.0}$	1267	not measured	
24	$Cu_{0.5}V_{0.5}Sr_2(Ca_{1.75}Sr_{0.25})Cu_3O_{9.7}$	1223, 1234	98,107	−12.9
25	$Cu_{0.5}V_{0.5}Sr_2(Ca_{1.75}Sr_{0.25})Cu_3O_{9.6}$	1234	107	−9.2
26	$Cu_{0.5}V_{0.5}Sr_2(Ca_{1.75}Sr_{0.25})Cu_3O_{9.5}$	1234	not measured	
27	$Cu_{0.5}V_{0.5}Sr_2(Ca_{2.15}Sr_{0.85})Cu_4O_{11.6}$	1234	107,90	−12.7
28	$Cu_{0.5}V_{0.5}Sr_2(Ca_{2.15}Sr_{0.85})Cu_4O_{11.3}$	1245, 1234	73,95	−7.93
29	$Cu_{0.5}V_{0.5}Sr_2(Ca_{3.6}Sr_{0.4})Cu_5O_{14.3}$	1234	not measured	
30	$Cu_{0.5}V_{0.5}Sr_2(Ca_{3.6}Sr_{0.4})Cu_5O_{14.0}$	1234	not measured	
31	$Cu_{0.5}V_{0.5}Sr_2(Ca_{3.6}Sr_{0.4})Cu_5O_{13.7}$	1256	75	−6.37
32	$Cu_{0.5}V_{0.5}Sr_2(Ca_{3.6}Sr_{0.4})Cu_5O_{13.6}$	1245, 1234	75,103	-7.58
33	$Cu_{0.5}V_{0.5}Sr_2(Ca_{3.6}Sr_{0.4})Cu_5O_{13.55}$	1245	75,101	-8.91
34	$Cu_{0.5}V_{0.5}Sr_2(Ca_{3.6}Sr_{0.4})Cu_5O_{13.5}$	1256	75	-7.52
35	$Cu_{0.5}V_{0.5}Sr_2(Ca_{3.6}Sr_{0.4})Cu_5O_{13.4}$	1256,1267	not measured	
36	$Cu_{0.5}V_{0.5}Sr_2(Ca_{3.6}Sr_{0.4})Cu_5O_{13.3}$	1256,1267	not measured	
37	$Cu_{0.5}V_{0.5}Sr_2(Ca_{4.7}Sr_{0.3})Cu_6O_{16.3}$	1245	not measured	
38	$Cu_{0.5}V_{0.5}Sr_2(Ca_{4.7}Sr_{0.3})Cu_6O_{16.0}$	1245, 1234	75,101	-5.8
39	$Cu_{0.5}V_{0.5}Sr_2(Ca_{4.7}Sr_{0.3})Cu_6O_{15.7}$	1245,1256	not measured	
40	$Cu_{0.5}V_{0.5}Sr_2(Ca_{4.7}Sr_{0.3})Cu_6O_{15.5}$	1256	75, 95	−6.44
41	$Cu_{0.5}V_{0.5}Sr_2(Ca_{4.7}Sr_{0.3})Cu_6O_{15.4}$	1267	75	−3.95
42	$Cu_{0.5}V_{0.5}Sr_2(Ca_{4.7}Sr_{0.3})Cu_6O_{15.3}$	1267	75	−4.86
43	$Cu_{0.5}V_{0.5}Sr_2(Ca_{4.7}Sr_{0.3})Cu_6O_{15.2}$	1267	not measured	
44	$Cu_{0.5}V_{0.5}Sr_2(Ca_{4.7}Sr_{0.3})Cu_6O_{15.1}$	1267	not measured	
45	$Cu_{0.5}V_{0.5}Sr_2(Ca_{5.7}Sr_{0.3})Cu_7O_{17.3}$	1256	75	−5.48
46	$Cu_{0.5}V_{0.5}Sr_2(Ca_{5.7}Sr_{0.3})Cu_7O_{17.2}$	1267	65	−0.03
47	$Cu_{0.5}V_{0.5}Sr_2(Ca_{6.7}Sr_{0.3})Cu_8O_{19.2}$	1267	75	−2.47
48	$Cu_{0.5}V_{0.5}Sr_2(Ca_{2.3}Sr_{0.7})Cu_4O_{11.6}$	1234	107	−12.5
49	$Cu_{0.5}V_{0.5}Sr_2(Ca_{4.55}Sr_{0.45})Cu_6O_{15.3}$	1267	75	−3.93
50	$Cu_{0.5}V_{0.5}Sr_2(Ca_{5.4}Sr_{0.6})Cu_7O_{17.3}$	1267	75	−4.89

[a] Only superconducting (Cu,V)−12($n-1$)n−Sr phases are shown using a simple abbreviation, 12($n-1$)n. [b] Magnetic susceptibility at 5 K.

2. Experimental Section

V_2O_5 (99.9%), $SrCuO_2$, SrO_2, Ca_2CuO_3, and CuO (99.9%) were used to obtain nominal mixtures for high-pressure synthesis. $SrCuO_2$ and Ca_2CuO_3 were prepared through solid-state reaction of CuO and $SrCO_3$ (99.9%) or $CaCO_3$ (99.9%) at 1000 °C for 5 days with several intermediate grindings. SrO_2 was prepared through a solution route.[13] These materials were confirmed to be free from impurity phases by X-ray powder diffraction (XRD) measurements. The cation ratios in the mixtures were adjusted to $(Cu_{0.5}V_{0.5})Sr_2(Sr,Ca)_{n-1}Cu_nO_y$ ($n = 3-7$) by varying the oxygen content, y, by changing the ratios between $SrCuO_2$, SrO_2, and CuO. The mixtures were sealed in gold capsules after being pulverized well and allowed to react in a belt-type high-pressure apparatus at 6 GPa and 1300 °C. After heat treatment for 1 h, the samples were quenched to room temperature, and then the pressure was released. To check possible oxygen loss, the gold capsules were weighed before and after the experiments.

The XRD data was collected by a diffractometer (Philips, PW1800) with Cu Kα radiation over the range $2\theta = 2-70°$. The lattice parameters were determined by least-squares refinements. Electron diffraction (ED) patterns and lattice images were taken using a Hitachi H-1500 high-resolution transmission electron microscope (HRTEM) operated at 800 kV. Electron-probe microanalysis (EPMA) was carried out using a JEOL JXA-8600MX analyzer. In EPMA, a small ceramic specimen was well polished to obtain a surface with $\approx 2 \times 2$ mm^2, and 5−10 relatively large grains were selected for each specimen.

The magnetic susceptibilities were measured as a function of temperature under zero-field-cooling and field-cooling conditions in an applied field of 20 Oe using a commercial DC SQUID magnetometer (Quantum Design, MPMS). The electric resistivity measurements were made via the conventional DC four-probe method with silver paste as an electrode using a physical property measurement system (Quantum Design, PPMS).

3. Results and Discussion

Table 1 summarizes all synthesis experiments including starting compositions, superconducting phases identified in the high-pressure products, and their super-

---

(13) Isobe, M.; Matsui, Y.; Takayama-Muromachi, E. *Physica C* **1996**, *273*, 72.

conducting properties. The T_c in the table is the value determined from the magnetic susceptibility data collected by the zero-field-cooling method. When a sample showed two-step decreases of the susceptibility, T_c corresponding to the major decrease is listed first and that corresponding to the minor decrease second, although the phase corresponding to the minor decrease was not sometimes detected by XRD due to its small volume fraction. In addition, the magnetic susceptibility at 5 K by the zero-field cooling method is given as a rough measure of the superconducting volume fraction.

As the preliminary experiment, we tested "stoichiometric" stating mixtures $(Cu_{0.5}V_{0.5})Sr_2Ca_{n-1}Cu_nO_y$ with $1 \leq n \leq 4$ (samples of nos. 1-2 and 5-23). Starting oxygen content y is an important parameter as well as the cation contents, and its delicate control is needed to prepare a desired superconducting phase.[1] It is experimentally observed and generally accepted for hole-doped cuprate superconductors that the optimum formal copper valence lies between 2.1+ and 2.2+. This fact was helpful to decide the range of the oxygen content to be tested since we could estimate the average copper valence of the present system for a given y value assuming the pentavalent state of vanadium. As shown in Table 1, the oxygen content was varied for each n according to this guideline.

Although the X-ray diffraction patterns of the "stoichiometric" samples were quite complicated implying multiphase coexisting states,[12] we could confirm presence of M−12(n − 1)n−A type phases with n = 3−7 because lattice parameters of a tetragonal M−12(n − 1)n−A phase obey a general relation, a (Å) ≈ 3.9 and c (Å) ≈ 3.2(n − 1) + constant where 3.9 and 3.2 Å reflect the in-plane size of the CuO_2 plane and the thickness of the $Ca-CuO_2$ composite planes, respectively.[1,2] Dominant impurity phases included in these samples were the incommensurate $(Ca,Sr)_{1-x}CuO_2$ compound[14−17] and the infinite-layer $(Ca,Sr)CuO_2$ compound.[18,19] In Table 1, it is often seen that a superconducting phase formed from a "stoichiometric" mixture has an n value different from a nominal value; for instance, n = 2 starting mixtures resulted in formation of n = 3, 4, 5 phases. This fact suggests that real cation compositions differ from the "stoichiometric" ones. To determine cation compositions in superconducting phases experimentally, four samples were selected and analyzed by EPMA. Table 2 gives the EPMA data for n = 3, 4, 5, 6 phases in samples with nominal compositions: $(Cu_{0.5}V_{0.5})Sr_2CaCu_2O_{7.5}$ (no. 6), $(Cu_{0.5}V_{0.5})Sr_2CaCu_2O_{7.15}$ (no. 8), $(Cu_{0.5}V_{0.5})Sr_2Ca_2Cu_3O_{9.4}$ (no. 13), and $(Cu_{0.5}V_{0.5})Sr_2Ca_3Cu_4O_{11.4}$ (no. 20), respectively.

Table 2. EPMA Data for the (Cu,V)−12(n − 1)n−Sr Phases

		atomic ratio					
		Ca/Sr		Cu/(Ca + Sr)		V/(Ca + Sr)	
n	no.[a]	obsd	calcd[b]	obsd	calcd[b]	obsd	calcd[b]
3	6	0.77(1)[c]	1.0	0.86(9)	0.875	0.09(4)	0.125
4	8	0.75(3)	1.5	0.88(7)	0.9	0.08(5)	0.1
	27	0.86(3)		0.87(9)		0.08(1)	
5	13	1.51(5)	2.0	0.89(2)	0.917	0.07(4)	0.083
	33	1.86(4)		0.91(4)		0.06(1)	
6	20	2.07(5)	2.5	0.89(9)	0.929	0.06(2)	0.071
7	42	2.10(8)	3.0	0.92(4)	0.937	0.04(6)	0.063

[a] Sample number used in Table 1. [b] Calculated from the $(Cu_{0.5}V_{0.5})Sr_2Ca_{n-1}Cu_nO_y$ composition. [c] Experimental error in parentheses is applied to the last digit.

In Table 2, the Ca/Sr ratio observed is always much smaller than (n − 1)/2 which is expected for the ideal composition $(Cu_{0.5}V_{0.5})Sr_2Ca_{n-1}Cu_nO_y$ and implies partial substitution of strontium for calcium. On the other hand, both Cu/(Sr + Ca) and V/(Sr + Ca) ratios are consistent with the ideal composition having values close to (n + 0.5)/(n + 1) and 0.5/(n + 1), respectively. According to these results, we tested various Sr-rich nominal compositions $(Cu_{0.5}V_{0.5})Sr_2(Ca,Sr)_{n-1}Cu_nO_y$ (nos. 24−47 in Table 1). This attempt was quite successful as we were able to isolate the n = 3−7 phases as almost single phase.

Figure 1 shows the XRD patterns of high-pressure samples with nominal compositions of $(Cu_{0.5}V_{0.5})Sr_2(Ca_{1.75}Sr_{0.25})Cu_3O_{9.7}$ (no. 24), $(Cu_{0.5}V_{0.5})Sr_2(Ca_{2.15}Sr_{0.75})Cu_4O_{11.6}$ (no. 27), $(Cu_{0.5}V_{0.5})Sr_2(Ca_{3.6}Sr_{0.4})Cu_5O_{13.55}$ (no. 33), $(Cu_{0.5}V_{0.5})Sr_2(Ca_{3.6}Sr_{0.4})Cu_5O_{13.5}$ (no. 34) and $(Cu_{0.5}V_{0.5})Sr_2(Ca_{4.7}Sr_{0.3})Cu_6O_{15.3}$ (no. 42). These samples contain n = 3, 4, 5, 6, 7 phases as a major component, respectively, and each X-ray pattern can be assigned by assuming a simple tetragonal lattice with the lattice parameters presented in Table 3. The lattice parameters show the general relation as a (Å) ≈ 3.85 and c (Å) ≈ 8.3 + 3.2(n − 1).

To confirm the phase identification, the aforementioned samples were observed by HRTEM. Figure 2 shows typical $hk0$ and $h0l$ ED patterns which were obtained for the n = 4 phase. These patterns are consistent with primitive tetragonal cells of possible space group $P4/mmm$. Similar simple ED patterns without any superstructure spots were observed for other members with n = 3−7. In the (Cu,M′)-series of phases, copper and M′ elements in the (Cu,M′) plane are often arranged as Cu−M′−Cu−M′... to give a 2a superlattice when M′ is a nonmetal element such as carbon, sulfur, phosphorus, etc.[1] On the contrary, for a metal M′ element such as germanium or chromium, this ordering dose not occur and Cu and M′ are placed randomly.[1] The simple ED patterns of the present (Cu,V) series of phases indicate that copper and vanadium in the (Cu,V) plane are also arranged randomly.

Parts a−c of Figure 3 show typical HRTEM images projected along the b-axis for the n = 3, 4, 6 phases. All these images are consistent with the M−12(n − 1)n-type structures with M = (Cu,V) and stacking of planes of $SrO-(Cu,V)O-SrO-CuO_2-(Ca-CuO_2)_{n-1}$. Any ordering in copper and vanadium in the (Cu,V) plane was not observed in the images, consistent with the ED patterns. From the XRD measurements, we confirmed presence of the (Cu,V) phases up to n = 7. In the HRTEM study, however, we sometimes observed a higher order phase with n = 8 as its $h0l$ ED pattern and lattice image are shown in Figure 3d. This fact

---

(14) Ross, R. S.; Rawn, C. J.; Ritter, J. J.; Burton, B. P. *J. Am. Ceram. Soc.* **1989**, *72*, 1545.

(15) Siegrist, T.; Ross, R. S.; Rawn, C. J.; Ritter, J. J. *Chem. Mater.* **1990**, *2*, 192.

(16) Sastry, P. V. P. S. S.; Robertson, A. D.; Lachowski, E. E.; Coats, A.; West, A. R. *J. Mater. Chem.* **1995**, *5*, 1931.

(17) Karpinski, J.; Schwer, H.; Meijer, G. I.; Conder, K.; Kopnin, E. M.; Rossel, C. *Physica C* **1997**, *274*, 99.

(18) Siegrist, T.; Zahurak, S. M.; Murphy, D. W.; Roth, R. S. *Nature* **1988**, *334*, 231.

(19) Takano, M.; Takeda, Y.; Okada, H.; Miyamoto, M.; Kusaka, T. *Physica C* **1989**, *159*, 375.

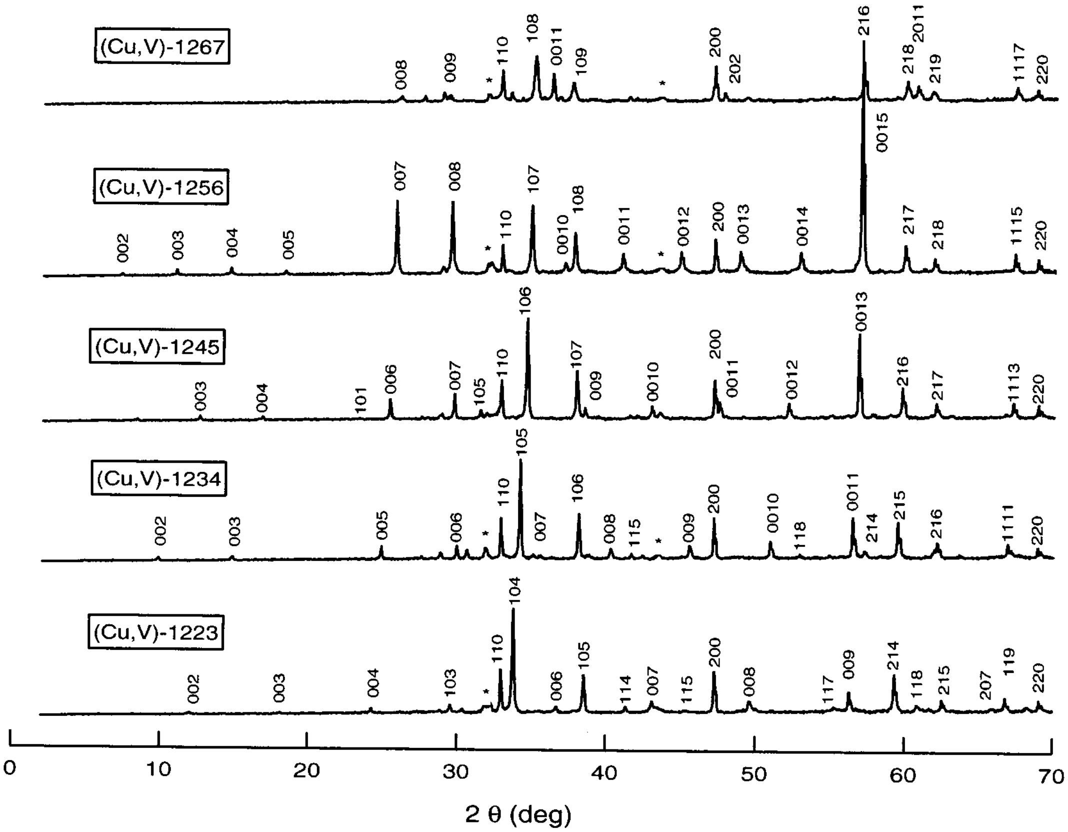

Figure 1. X-ray powder diffraction patterns of samples of nos. 24, 27, 33, 34, and 42 in Table 1 which are denoted as (Cu,V)−1223, −1234, −1245, −1256, and −1267, respectively. Peaks marked by an asterisk belong to the incommensurate $(Ca,Sr)_{1-x}CuO_2$ compound.

Table 3. Lattice Parameters, Cell Volumes, and T_c of the (Cu,V)−12(n − 1)n−Sr Phases

n	no.[a]	a (Å)	c (Å)	V (Å^3)	T_c (K)[b]
3	24	3.8418(4)[c]	14.691(2)	216.83(5)	98
4	27	3.8497(3)	17.900(1)	265.28(4)	107
5	33	3.8498(3)	21.036(2)	311.77(6)	75
6	34	3.8532(6)	24.226(3)	359.7(1)	75
7	42	3.8572(6)	27.434(7)	408.2(1)	73

[a] Sample number used in Table 1. [b] T_c determined by the magnetic susceptibility measurement. [c] Experimental error in parentheses is applied to the last digit.

suggests strongly that we can synthesize the $n = 8$ phase in bulk form by controlling the synthesis condition, and such a experiment is in progress.

Intergrowth of a phase with a different n value is a crystal defect often observed in the layered superconductor structures, especially in high n members. However, few intergrowth defects are seen in the HRTEM images in Figure 3 and stacking sequence of planes along the c-axis is quite regular even in the $n = 8$ member. Similar phenomenon was reported for the (Cu,Cr)−12(n − 1)n−Sr series[2] whereas intergrowth formation is far more pronounced in other series of phases such as (Cu,P)−12(n − 1)n−Sr and (Cu,S)−12(n − 1)n−Sr.[1] The suppression of the intergrowth defect formation seems to be related to the fact that the superconducting phases are stabilized for a wide range of n in the (Cu,Cr) or (Cu,V) series, although we do not know yet which is the most important crystal chemical factor governing the intergrowth formation.

Some of the samples in Figure 1 still include the incommensurate $(Ca,Sr)_{1-x}CuO_2$ compound as an im-

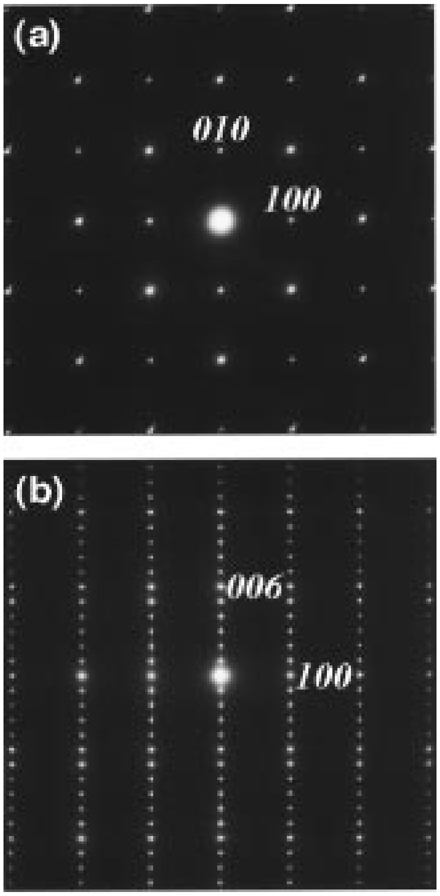

Figure 2. $hk0$ (a) and $h0l$ (b) ED patterns of the (Cu,V)−1234−Sr phase.

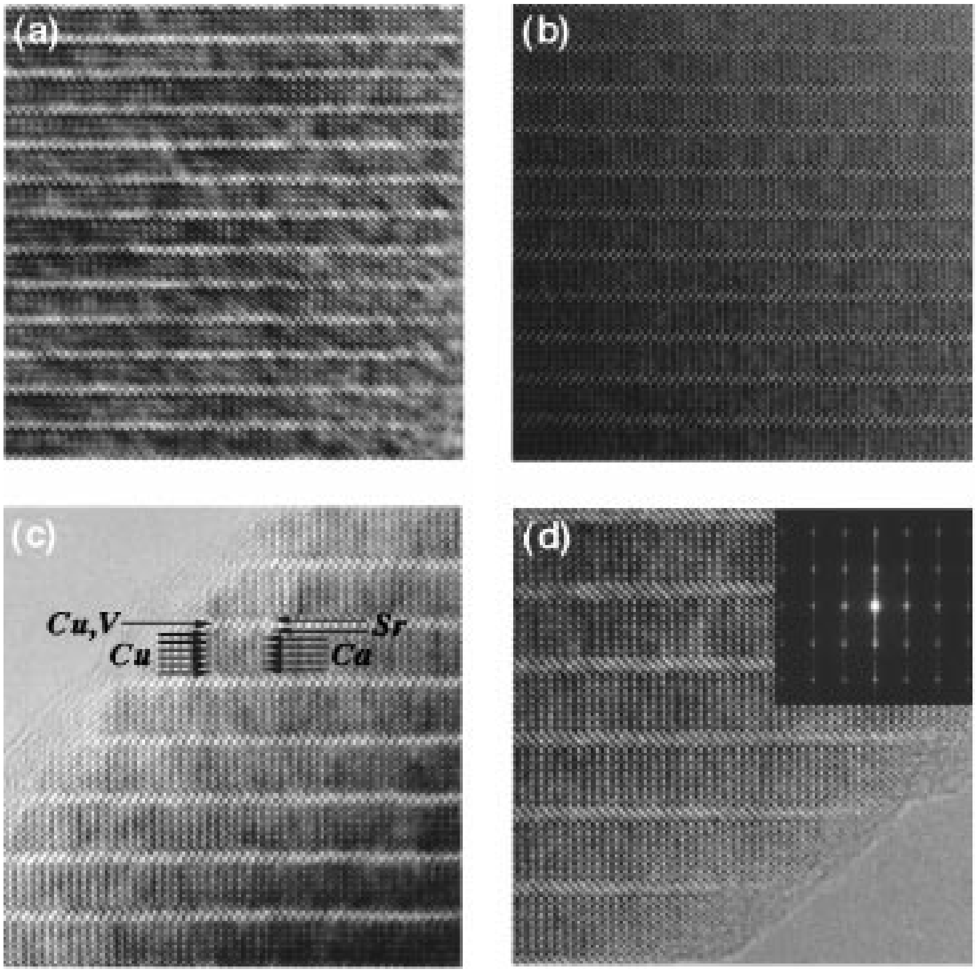

Figure 3. Lattice images projected along the *b*-axis for the $n = 3$ (a), 4 (b), 6 (c), and 8 (d) members of the (Cu,V)−12($n - 1$)n−Sr series. The insert in Figure 3d is the *h*0*l* ED pattern of the $n = 8$ phase.

purity phase as denoted by an asterisk in the figure. In addition, the $n = 6$ phase was formed from the $n = 5$ starting mixture (no. 34) and the $n = 7$ phase from the $n = 6$ starting mixture (no. 42). To solve these issues, we carried out once more EPMA measurements for $n =$ 4, 5, 7 phases in the samples of nos. 27, 33, and 42, respectively, with the results given in Table 2. The Cu/(Ca + Sr) and V/(Ca + Sr) ratios in the $n = 4$, 5 phases are not different between the two sets of samples obtained from the “stoichiometric” and the Sr-rich nominal compositions. On the other hand, the Ca/Sr ratios differ beyond experimental uncertainty, in particular, in the $n = 5$ phase. This result suggests that there exist solid solution ranges for Sr/Ca in the present (Cu,V)-based phases. We adjusted the starting nominal compositions to the new EPMA data and three nominal compositions (nos. 48, 49, and 50) were tested, but phase purity was not improved and the samples in Figure 1 are, at the present stage, our best ones for the $n = 3-7$ phases.

Vanadium can have various oxidation states in an oxide, 2+, 3+, 4+, or 5+, depending on oxygen fugacity in a synthesis system. In the present case, the (Cu,V) phases were prepared under very high oxygen-fugacity atmospheres and this synthesis condition suggests a pentavalent state of vanadium in the (Cu,V) phases. Although we need further investigations for a higher quality sample to confirm the oxidation state of the vanadium, it is worth noting that the oxidation state is less than or equal to 5+. On the other hand, chromium in the (Cu,Cr) phases was reported to be hexavalent, and no holes are created if we assume $Cu_{0.5}Cr_{0.5}O$ composition for the (Cu,Cr) plane.[2] Presence of excess oxygen and/or copper vacancy in the (Cu,Cr) plane was suggested as the hole-doping mechanism in the (Cu,Cr) phases.[2] In the present vanadium system, the (Cu,Cr) plane with $Cu_{0.5}V_{0.5}O$ composition will yield 0.5 hole per unit formula assuming the V^{5+} ion or a greater number of holes assuming an oxidation state less than 5+. Although crystal defects such as excess oxygen in the (Cu,Cr) plane should also be considered as origin of the hole carrier, “self-doping” of holes due to the vanadium ion seems to play an important role regarding to the carrier introduction.

Finally we discuss superconducting properties of the (Cu,V) phases. Figure 4 shows the zero-field-cooling susceptibility data of the samples of nos. 24, 27, 33, 34, and 42, which were the best samples for the $n = 3-7$ phases judging from the X-ray diffraction patterns, respectively. The no. 24 sample (denoted simply as 1223 in the figure) showed two-step steep decreases of susceptibility with a larger decrease at 98 K and a smaller decrease at 107 K. The 98 K transition is caused by the main phase with $n = 3$ whereas the 107 K transition is probably due to the presence of a small amount of the $n = 4$ phase as it was detected by XRD. The no. 5 and no. 6 samples become superconducting below 95 and 98 K, respectively (Table 1). Although

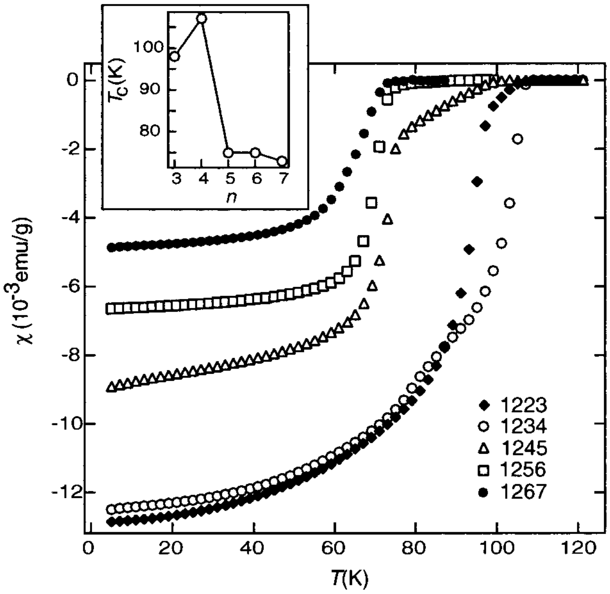

Figure 4. Zero-field-cooling susceptibility data of samples of nos. 24, 27, 33, 34, and 42 in Table 1 which are denoted simply as 1223, 1234, 1245, 1256, and 1267, respectively. The insert shows the T_c variation as a function of *n*.

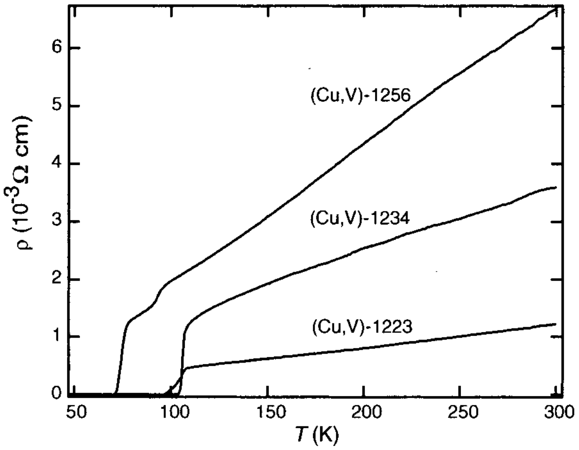

Figure 5. Dc resistivity data for the samples of nos. 24, 27, and 34 in Table 1 which are denoted as (Cu,V)−1223, −1234, and −1256, respectively.

these samples were less pure compared with the no. 24 sample, they contained only the $n = 3$ phase as a superconductor and their T_cs support the assignment of 98 K to the $n = 3$ phase. The no. 27 sample (1234) showed a sharp superconducting transition at 107 K which is attributed to the $n = 4$ phase. In addition, a small anomaly is seen near 90 K which may be attributed to the $n = 3$ phase although it was not detected in the X-ray pattern. According to Table 1, T_c of the $n = 4$ phase varies fairly largely depending on the nominal composition. For instance, the no. 8 sample, which contained only the $n = 4$ phase as a superconductor, showed T_c of 98 K while the samples with nos. 10, 11, 12, 25, and 27 showed T_cs ranging from 104 to 107 K.

The no. 33 sample (1245) showed two-step transitions at 75 and 101 K with the former as the main transition. Since this sample included the $n = 5$ phase as a major component, the 75 K transition was assigned to the $n = 5$ phase, and the 101 K transition appears to be caused by the $n = 4$ member included as a minor phase. The no. 13 sample contained only the $n = 5$ phase as a superconductor, and it become superconducting below 75 K, as well. The samples of nos. 34 (1256) and 42 (1267) showed single-step transitions at 75 and 73 K which are ascribed to the $n = 6$ and 7 phases, respectively. The T_c obtained for these particular samples does not present a smooth variation as a function of *n* but decreases largely between $n = 4$ and 5 and has an almost constant value for $n \geq 5$ (see the insert of Figure 4). The T_c depends not only on *n* but also on other factors such as the excess oxygen content and the cation ratios as seen previously and has a certain width at each *n*. We have not optimized T_c on these various synthesis parameters, as yet. However, the T_c variation in each phase of the present system seems not very large; it is ~2−10 K as suggested from Table 1.

Figure 5 shows temperature dependencies of the resistivities for the samples of nos. 24, 27, and 34 which are denoted as (Cu,V)−1223, −1234, and −1256 in the figure, respectively. Every sample shows superconducting transitions consistent with the magnetic susceptibility data in Figure 4. Every resistivity above T_c shows a metallic nature with a positive temperature dependence. If we assume a constant number of holes are created in the (Cu,V) plane throughout the series, the hole concentration or the average copper oxidation state would decrease linearly with increasing *n*.[1] As we can see in Figure 5, the normal-state resistivity indeed systematically increases with *n*, implying the decrease of the hole concentration with *n*. More quantitative discussion on the hole concentration is difficult at the present stage because we do not know exactly the oxidation state of copper in each superconducting phase. For this purpose, we need more than anything else to obtain a phase pure sample in the strict sense. Hole coefficient measurement for such a sample, for instance, would be useful to estimate the hole concentration.

4. Summary

A new series of V-based high T_c superconductors $(Cu,V)Sr_2Ca_{n-1}Cu_nO_y$ ($n = 3$−7) was synthesized under a high-pressure/high-temperature condition. They have tetragonal layered structures with a stacking sequence of planes, SrO−(Cu,V)O−SrO−$(Ca-CuO_2)_{n-1}$. The copper and the vanadium atoms in the (Cu,V) plane are placed randomly with their ratio V/Cu close to unity. The Ca/Sr ratio determined experimentally was generally smaller than the stoichiometric value of $(n - 1)/2$ indicating partial replacement of strontium for calcium. All the members of the series show superconductivity with T_c = 98, 107, 75, 75, 73 K for n = 3, 4, 5, 6, 7, respectively. The normal-state electric resistivity tended to increase with increasing *n*, implying the decrease of the hole concentration with *n*.

Acknowledgment. The authors wish to express their thanks to Drs. M. Akaishi and S. Yamaoka of NIRIM for their helpful suggestions on high-pressure synthesis. They also thank to K. Kosuda and K. Natori for technical assistance. This work was supported by the Multi-Core Project, the COE Project, the Special Coordination Fund of the Science and Technology Agency, and the Technical Specialist Supporting Program by the JRDC.

CM990109+